EKF based State Estimation of Power System including Solar PV based Generation

Major Project Report

Submitted in Partial Fulfillment of the Requirements

for the Degree of

MASTER OF TECHNOLOGY

IN

ELECTRICAL ENGINEERING

(Electrical Power Systems)

By

BANDITA SHARMA

13MEEE23

DEPARTMENT OF ELECTRICAL ENGINEERING

INSTITUTE OF TECHNOLOGY

NIRMA UNIVERSITY

AHMEDABAD-382481

MAY 2015

EKF based State Estimation of Power System including Solar PV based Generation

Major Project Report

Submitted in Partial Fulfillment of the Requirements

for the Degree of

MASTER OF TECHNOLOGY

IN

ELECTRICAL ENGINEERING

(Electrical Power Systems)

By

BANDITA SHARMA

13MEEE23

DEPARTMENT OF ELECTRICAL ENGINEERING

INSTITUTE OF TECHNOLOGY

NIRMA UNIVERSITY

AHMEDABAD-382481

MAY 2015

Undertaking For Originality of the Work

I, **Bandita Sharma (Roll No:**13**MEEE**23), give undertaking that the Major Project entitled **"EKF based State Estimation of Power System including Solar PV based Generation**" submitted by me, towards the partial fulfillment of the requirement for the degree of Master of Technology in Electrical Power Systems, Electrical Engineering, under Institute of Technology, Nirma University, Ahmedabad is the original work carried out by me and I give assurance that no attempt of plagiarism has been made. I understand that in event of any similarity found subsequently with any published work or any Dissertation work elsewhere; it will result in severe disciplinary action.

....

Signature of Student

Date:

Place: Ahmedabad

Endorsed By:

....

Project Guide

Dr. S.C. Vora

Department of Electrical Engineering

Institute of Technology

Nirma University

Ahmedabad

Certificate

This is to certify that the Major Project Report entitled **"EKF based State Estimation of Power System including Solar PV based Generation"** submitted by **Ms. Bandita Sharma (Roll No:13MEEE23)** towards the partial fulfillment of the requirements for the award of degree in Master of Technology (Electrical Engineering) in the field of Electrical Power Systems of Nirma University is the record of work carried out by him/her under our supervision and guidance. The work submitted has in our opinion reached a level required for being accepted for examination. The results embodied in this major project work to the best of our knowledge have not been submitted to any other University or Institution for award of any degree or diploma.

Date:

....

Project Guide

Dr. S.C. Vora

Department of Electrical Engineering

Institute of Technology

Nirma University

Ahmedabad

Head of Department

Department of Electrical Engineering

Institute of Technology

Nirma University

Ahmedabad

Director

Institute of Technology

Nirma University

Ahmedabad

Acknowledgement

"The success of any task lies upon the efforts made by a person but it cannot be achieved without the co-operation of others"

Foremost, I take this opportunity to express my profound gratitude and deep regards to my Guide **Dr. Santosh C.Vora Sir** for his exemplary guidance, monitoring and constant encouragement throughout the course of this thesis. I sincerely thank Sir for believing in me and giving me an opportunity to work with him. He has always guided me whole-heartedly which has motivated me throughout the period of dissertation work. The blessings, help and guidance given by him from time to time shall carry me a long way in the journey of life on which I am about to embark. His guidance has helped me throughout my study and writing of this thesis. I could not have found a better mentor and advisor for my M.Tech study.

I would like to express my gratitude to Dr. Vivek Pandya Sir for his constant motivation from my B.E. days. I would also like to give my sincere thanks to Ms. Meera Karamta Ma'am and Prof. Siddharth S.Joshi Sir for sharing their knowledge about the various topics of this work.

I am obliged to the staff members and the lab technicians of electrical department of Institute of Technology, Nirma University, for the valuable information provided by them in their respective fields. I am grateful for their co-operation during the period of my dissertation work. I also take this opportunity to express a deep sense of gratitude to my university for the cordial support provided in terms of the project lab, valuable information and guidance which helped me in completing this task through various stages.

Lastly, I thank the Almighty, my parents, brother, sister and my classmates for their constant encouragement without which this dissertation work would not have been completed.

Abstract

State Estimation is the most vital function of the energy management system(EMS) and aims at analysing, monitoring and controlling the stability of the electric power system. Reliability of the modern power system greatly depends on the fact that how efficient and accurate is the state estimation. Due to the slow updation rate of SCADA systems, the traditional state estimators which are based on steady sate system model cannot capture the system dynamics very well . Thus, to overcome these limitations, wide area measurements and control systems (WAMAC) using PMUs are being implemented worldwide. WAMAC systems have the ability to capture dynamic system information which is beneficial for the state estimators of a power system in generating dynamic states i.e. synchronous generator rotor angle and synchronous generator speed giving an accurate picture of the overall condition of power network thereby leading to an enhanced situational awareness by the system operators.

Moreover, though the power system planners have a variety of generation technologies to chose from, there is an increasing interest in the use of renewables. Due to excellent solar resource availability, it is intended to replace one of the synchronous generators by PV array in order to generate the adequate amount of power. Based on this point of view, changes taking place in the system dynamics due to penetration of solar into the grid is intended to be studied and estimated. The modeling of the system is carried out on standard WSCC 3- generator, 9-bus system in MATLAB®. As a whole, the dynamic state estimation process is laid out based on Extended Kalman Filtering Technique.

Abbreviations

SE .... State Estimation
SSE .... Static State Estimation
DSE .... Dynamic State Estimation
EKF .... Extended Kalman Filter
SCADA .... Supervisory Control And Data Aquisition
PMU .... Phasor Measurement Unit
WSCC .... Western System Co-ordinating Council
EMS .... Energy Management System

Superscripts

$\hat{}$ .... estimated value notation
$^-$ .... a priori estimate

List of Figures

List of Tables

Contents

Chapter 1

Introduction

The design and operation of electrical power systems is given greater importance due to its high complexity. In the present scenario, almost all the power systems are undergoing effective changes throughout the world. As stated under the open-access regulations, it is a pre-requisite for all the transmission owners to open their systems so that other entities can use it, including many non-utility entities. Earlier, the transmission systems were considered as a link to connect the generation and the distribution systems. But, the present day scenario is such that the transmission system has become an electricity market trading floor. Most of the competitors in the market aims towards achieving commercial goals rather than the technical ones. Due to this present day scenario, the power grid is facing many challenges.

Among the various challenges that the present day power system computer applications have to solve, some of them are listed below:

- new and unexpected situations
- unpredictable changes in the power flow due to unusual modes of energy trades
- multiple possibilities of fault to occur affecting the reliability of the system

Computation techniques are now used almost in all the aspects of the power system. To operate reliably, robustly and efficiently, the new restructured system requires more engineering and financial background. The market participants demands the dynamic information about the physical system state, past, present, and forecast. A need of the hour is to possess a real-time model resembling the current situation on which the power network computations can be performed. Real-time model means a “snapshot” of the system containing redundant measurements of the quantities of interest, the exact scheme from which the measurements are derived and the accurate parameters of the elements in the model. A collection of measured data and computer applications for monitoring and control of the power network is provided by the Energy Management System (EMS). The supervisory control and data acquisition(SCADA)system helps in monitoring and controlling the power system assets. Earlier, it was understood that the real-time data base provided by SCADA provides an accurate view of the system to the operator but, the inaccuracies in the SCADA system were realized at a later stage. Some of the deficiences of the SCADA system are:

- Difficulty in assuring whether all the measurements will be available at all times or not.
- Erroneous measurements

Therefore, a more powerful technique was needed to process the measurements that were collected and to filter the bad data. This was done by State Estimation (SE). State Estimation provides the accurate estimate of the state of the system which is based on a set of measurements of the model of the system. Variables of interest indicate the:

- margins to operating limits
- health of the equipment
- required operator action

State estimators are capable of calculating these variables of interest despite of:

- Measurements that are corrupted by noise
- Measurements that may be missing or inaccurate

State Estimation is broadly classified as: Static State Estimation And Dynamic State Estimation. The main objective of this project is to study in detail about the Dynamic State Estimation considering Solar as the source of renewable energy.

1.1 Literature Survey

For carrying out the dissertation work on any topic, having in depth knowledge about the concepts is of prime importance. This knowledge is achieved by reading the wide literature available. This section describes about some of the IEEE papers read to understand the concept of dynamic state estimation and the various techniques used in this.

- **Amit Jain and Shivkumar N.R.**[1]: This is a review paper which describes the importance of Tracking State Estimation in power system. Various techniques have been proposed to improve the computability, accuracy and the ease of implementation. The authors have made an attempt to compare Tracking State Estimation with Dynamic State Estimation and have proven the latter one to be more efficient. Various DSE Techniques have been proposed and the advantages and the disadvantages of the same has been reflected.

- **Amit Jain and Shivkumar N.R.**[2]: This review paper describes the importance of PMUs in DSE of Power System and proves it to be accurate in measuring the voltage and current phasors. The authors have presented a case wherein a comparison between the use of a single PMU and Multiple PMUs has been done. This paper shows that PMUs are extremely accurate measuring devices with the capability of reducing the errors in the estimates of the DSE.

- **Jun Zhu and Ali Abur**[3]: With the advent of PMUs, the benefit of eliminating the reference phasor in processing the bad data has been discussed in this paper. It also illustrates the merging of observable islands using PMUs. The authors have proposed a rectangular coordinate formulation through which the numerical problems encountered while using current phasors can be avoided.

- **Benjamin Genet and Jean-Claude Maun**[4]: This paper proposes a new monitoring method based on wide area network of PMUs which gives a dynamic view of the system and allows the operator to locate the weakest node or area. The author aims to implement this method by installing PMUs in the part of the power system which is sensitive to voltage instability.

- **A.K. Sinha and J.K. Mondal**[5]: This paper basically gives the comparison between the conventional DSE method and DSE using ANN for load forecasting and it has been proved that the latter one gives the best state estimation. Though the computational time required for both is almost the same, ANN based dynamic load prediction is more accurate than the conventional one. The proposed scheme was tested on a large number of standard systems and was proved to be the best due to the inclusion of non-linearities in case of large changes in loads or generation.

- **Zhenyu Huang, Kevin Schneider and Jarck Nieplocha**[6]: This paper reveals that that complete dynamics of the system cannot be represented with voltage magnitudes and phase angles only. The generator rotor angles and the generator speeds has to be included for the complete analysis. EKF algorithm has been applied for the analysis of multi-machine system under large and small disturbances at some of the buses. EKF method proves to be more accurate for rejection of noise and disturbance conditions.

1.2 Problem Identification

As SCADA system can only take a few non-synchronized measurements in a second, most of the studies on SE has been focused on SSE for the last few decades. Furthermore,the new value of estimates are usually taken once in every few minutes in order to reduce the complexities in computer techniques required in implementing SE. Hence, for providing the real-time monitoring of the power network, SSE is not widely used. Conventional SCADA measurements are obtained very infrequently for capturing the dynamics of the power system completely. As the controller has very little time to respond when faults occur, it causes a serious challenge for the operators. Moreover, the possibility of unexpected changes in the system increases when the renewable energy sources in distributed generation (DG) are integrated in the system. Thus, it is necessary to note these changes from time to time to ensure the dependability and reliability of the power system. This arises the need of SE schemes that are able to capture and track the dynamics of the system which closely matches the real-time dynamics of the power system. This is the major drawback of the static state estimation techniques indicating that they are not sufficient for real time analysis of the system. Thus, Dynamic State Estimation which is capable of monitoring and controlling the system at the time of any contingency is the need of the hour. Moreover using Solar as a source of generation in place of a synchronous generator has the biggest advantage of saving the conventional sources of energy from getting deteriorated thereby making it available for future use.

1.3 Objective and Scope of the Project

The objective of this project work is to understand the Dynamic State Estimation approach thoroughly so that the operation of the power system can be analysed in a much efficient manner. This work is carried out to understand the performance of Extended Kalman Filtering Technique on a system. The performance of the system when Solar is included as a source of generation in place of a conventional synchronous generator has to be evaluated and studied. To achieve the objective of this project, the **scope of the work** is outlined as:

- Develop a standardized model of WSCC 3-generator, 9-bus system in a software and to observe load flow analysis under steady state condition.
- Gather information for active power, reactive power, voltage and load angle at each bus.
- Implement a specific model i.e. a Solar system with necessary power electronics and connecting this model into the grid in place of equivalent capacity synchronous generator in the WSCC system.

- Re-capture active power, reactive power, voltage and load angle at each bus with change of generator.
- Add noise to the above information with low noise (with variance of 10%).
- To Use EKF technique as a state estimator.
- To observe the simulation results and compare it with the results of conventional 3-generator, 9-bus system.

1.4 Organization of Thesis

The work carried out during the dissertation work is divided into four chapters. The present chapter gives a scenario of the various problems occurring in power grid thus introducing the need to carry out state estimation. It introduces the SSE and DSE and tells how DSE is better than SSE thus defining the motivation of the project. It also includes review of literature studied, problem identified and the scope of work.

- **Chapter 2** gives a brief description about how state estimation came into existence its concept.In this chapter, emphasis has been made on DSE. It describes the widely preferred DSE technique i.e. EKF in detail along with some of it benefits and limitations. It also describes about the technical requirements when a renewable source has to be connected with a system consisting of synchronous generator.
- **Chapter 3** includes the simulation work carried out. Results of simulation of the WSCC 3 generator 9 bus system under steady-state conditions and results of the system when one of the synchronous generator is replaced by a solar source are given. It includes the system modeling for WSCC system, system modeling when renewable source is included and the matrix for WSCC system for EKF to be implemented. Analysis of the obtained results are presented.
- **Chapter 4** comprises of conclusion and future work.

Chapter 2

Basic Concepts

2.1 Evolution of State Estimation

The phase angles and the magnitude of voltages at every bus determine the state of a power system. Using this information, along with the information regarding the topology and impedance parameters of the grid, the behaviour of the entire system can be analyzed. The SCADA system is a set of computation technique which is used to monitor, control and optimize the performance of a power system. SE is the most essential constituent here. The data acquisition system accepts the measurement from devices like Remote Terminal Units (RTUs) and now $PMU's$. The system state is calculated and the necessary information to the supervisory control system is provided by the state estimator, which then takes the necessary action by sending control signals to the circuit breakers. There are four main processes in the conventional state estimator and is shown in Fig. 2.1. The topology processor tracks the network topology and maintains a real-time database of the network. To ensure that the set of measurements taken are sufficient to execute SE, the process of observability analysis is carried out. Further, the major errors in the measurement set are identified and eliminated by the bad-data processor. Thus, the state estimator calculates the system state considering the set of high accuracy measurements.[6]

The SE technique may be further divided into two basic different concepts, depending on the timing and evolution of the estimates: Static SE (SSE) and Dynamic SE (DSE).

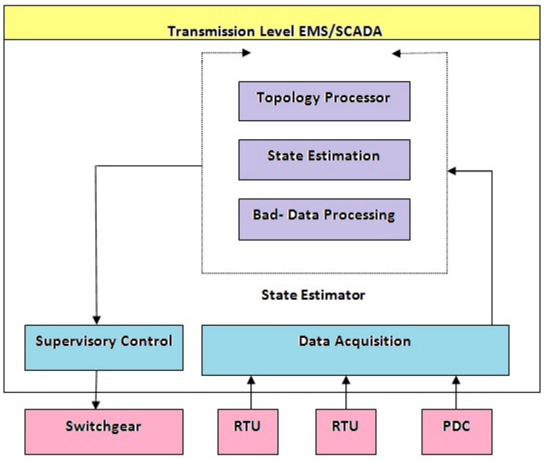

Figure 2.1: Block Diagram of SCADA

In this dissertation work, entire emphasis is given on DSE.

2.1.1 Dynamic State Estimation

As Static state estimation assumes the system to be quasi-static, it is performed by taking snapshots of measurements. This makes the analysis as a static analysis but in reality, power system is never constant. It changes with time and requires continuous monitoring and controlling as the rate at which transients occur in a system is faster than the rate at which measurements are taken. In such a case static state estimation is insufficient and requires heavy computing resources. Thus, there is a need for Dynamic State Estimation. DSE uses the present state of power system along with the knowledge of the system's physical model, to estimate present state (out of noisy measurements) and to predict the state vector for the next time instant. This prediction feature of DSE provides vital advantages in system operation, control and decision making.

The purpose of implementing DSE is to calculate the dynamic states of the power system, which are the state variables representing the power system in the form of non-linear differential-algebraic equations. Some of the dynamic states have to be computed as all the dynamic states are not directly measured. As the measurements are corrupted by noise, traditional observer technology cannot be directly applied. This is achieved by the use of Kalman filter techniques which functions as an effective tool for addressing many engineering issues. It has the ability to integrate noise characteristics into the computations. The Extended Kalman Filter (EKF) has been introduced for dealing with non-linear equations.

2.1.2 Various Techniques of Dynamic State Estimation

Dynamic State Estimation can be performed by the following methods:

- Kalman Filtering Based Techniques
    a. Extended Kalman Filtering
    b. Unscented Kalman Filtering
- PMU based DSE

In this dissertation work, main emphasis is given on EKF technique.

2.2 Extended Kalman Filter Technique

The conditional probability density functions providing the minimum mean-square estimate no longer remains Gaussian if any of the system state dynamics or the observation dynamics is non-linear. A non optimal approach to solve the problem, in the frame of linear filters, is the EKF. The EKF implements a kalman filter for a system dynamics that results from the linearization of the original non-linear filter dynamics around the previous state estimates[6].

2.2.1 Overview of Extended Kalman Filter

A dynamic system can generally be modelled as a set of non-linear differential equations[7]:

$$\dot{x} = dx/dt = f(x, y) \tag{2.1}$$

where x vector represents the state variables and the y vector represents the algebraic variables. The discrete form of equation 2.1 can be written as[7]:

$$x_k = x_{k-1} + f(x_{k-1}, y_{k-1})\Delta t \equiv g(x_{k-1}, y_{k-1}) \tag{2.2}$$

where k is the time step number and Δt is the time step[7]. Measurements at time step k can be represented as a vector of nonlinear functions h composed of the state variables x and measurement noise v[7]:

$$z_k = h(x_k, v_k) \tag{2.3}$$

The results error between the measured and calculated values is given by[7]:

$$\varepsilon_k = z_k - h(x_k, v_k) \tag{2.4}$$

The EKF is a two-step predicion-correction process. The prediction step is a time update using the difference equation 2.2, which predicts the state variables of the next step, x_k. In addition to the prediction of the state variables, a priori estimated error covariance is also predicted. The correction step takes the measurement z_k and uses the error ε_k calculated from equation 2.4 to correct state variables, x_k[7].
The equations for EKF are given as:

Prediction:

$$\begin{aligned} \hat{x_k}^- &= \hat{x}_{k-1} + (dx/dt)|_{k-1}\Delta t \\ &= \hat{x}_{k-1} + f(\hat{x}_{k-1}, z_{k-1})\Delta t \\ P_k^- &= A_k P_{k-1} A_k^T + W_k Q_{k-1} W_k^T \\ &= A_k P_{k-1} A_k^T \end{aligned} \tag{2.5}$$

Correction:

$$
\begin{aligned}
K_k &= P_k^- H_k^T (H_k P_k^- H_k^T + V_k R_k V_k^T)^{-1} \\
\hat{x}_k &= \hat{x_k}^- + K_k(z_k - h(\hat{x_k}^-, 0)) \\
P_k &= (1 - K_k H_k) P_k^-
\end{aligned}
\tag{2.6}
$$

where K is the Kalman gain matrix, P is the estimation error covariance matrix and A, H and V are jacobian matrices. The R matrix is the measurement error covariance matrix and needs to be tuned if the contribution due to measurement noise is not known. Larger values of R place more weight on the predicted value while smaller values of R place more weight on the measured values[7].

$$A = \partial g/\partial x \ \ , H = \partial h/\partial x \ \ , V = \partial h/\partial v \tag{2.7}$$

2.2.2 Reasons for using EKF as the State Estimator in the project

- Complete dynamics of the power system can be included in the process which ensures an accurate way for representing the changing states in the system.
- Its performance is superior in both the small disturbance condition and large disturbance condition.
- It has high level of sensitivity, detecting even the small noise level.

2.2.3 Disadvantages of Extended Kalman Filtering Technique

- Deriving the jacobians is a tedious job in most cases.
- Observability problems arises whenever the variables do not map onto each other.

- Singularity within functions can result into non-positive solutions and lead to instability.

2.3 Technical Aspects of Interconnection

A renewable energy source connected to the network consists of a locally available energy source, for example solar radiation, a device for converting this energy into AC electrical power which may include a DC-AC inverter, loads, and a point of common coupling where the equipment belonging to the client interfaces with the distribution system of the local power company. When a distributed electric production resource has to be connected with a grid, a number of technical challenges have to be faced by both renewable energy grid operator and the utility. These challenges may be:

- Maintenance of frequency and voltage.

- Coordinate the operation of reclosing of breakers and protective relays.

To interconnect a renewable energy source, it should satisfy the following requirements:

- It should be able to connect safely to the network at acceptable frequency and phase.

- To meet the utility requirements, it should be capable of injecting power of desired quality.

- It should be able to disconnect quickly and safely from the grid as soon as any disturbance is detected.

- It should be able to reconnect easily to the grid whenever it is safe to do so.

2.3.1 Interconnection requirements for a Synchronous Generator

Since the frequency of the output is directly proportional to the rotational speed of the rotor at a given speed in a synchronous generator, it will always produce the same frequency. Due to their ability to self start without the need of internal and external supply of reactive power, they are widely used[8].
Before connecting to the grid, there are certain requirements which are to be fulfilled. These are:

- The output voltage of the synchronous generator must be same as the mains voltage.
- The frequency of the incoming generator and the grid must be the same.
- Phase sequence must be same.

2.4 Summary

The overall idea of state estimation has been presented here. The purpose of using dynamic state estimation has been described in this chapter. EKF to be used as a state estimator has been explained in detail. The subsequent chapters make use of this background for simulations. This chapter also gave a brief idea about the complexities included when a small grid such as PV is integrated with a larger grid consisting of synchronous generator. It also tells about the interconnection requirements of a synchronous generator.

Chapter 3

Simulation Results

3.1 Description of WSCC 3-Generator 9-Bus System

To analyse the stability of a system, an appropriate standard model which is desired to be chosen so that comparison of the results can be done. So, in this project work the WSCC 3-generator, 9-bus system is taken as the standard model and future work is to be carried out in this system only.

The system is simulated using PSCAD and MATLAB® software and discussion in this report is based on the results obtained in MATLAB®. The base MVA is taken as 100MVA and the system frequency is 60Hz. The data required for the system is taken from references [9] and [10].

The first step is to simulate the system under steady state conditions. Using the load flow bus tool of MATLAB®, load flow of the system is computed which gives the results of the system under steady state (as expected in literature). The steady state results of the real and reactive power of the three generators are obtained.

3.1.1 The Model and Subsystems developed in MATLAB and their Simulation Results

The WSCC system is widely used in power system studies for testing the results. After studying a series of research papers based on the above system, the overall functioning of the system can be easily understood. Moreover, when a work has to be proved, it can be done only if we have a standard data from where the calculated and the simulated results can be verified. Thus, WSCC system is used for the analysis of various issues in this dissertation work.

The WSCC system consists of three generators among which generator 1 is a swing bus, generator 2 and 3 are PV buses. The governor and the excitation systems are included in the system to take care of the overall dynamics of the system. The data to be entered in the various components of the system are given in the following tables. All the results obtained are in p.u.

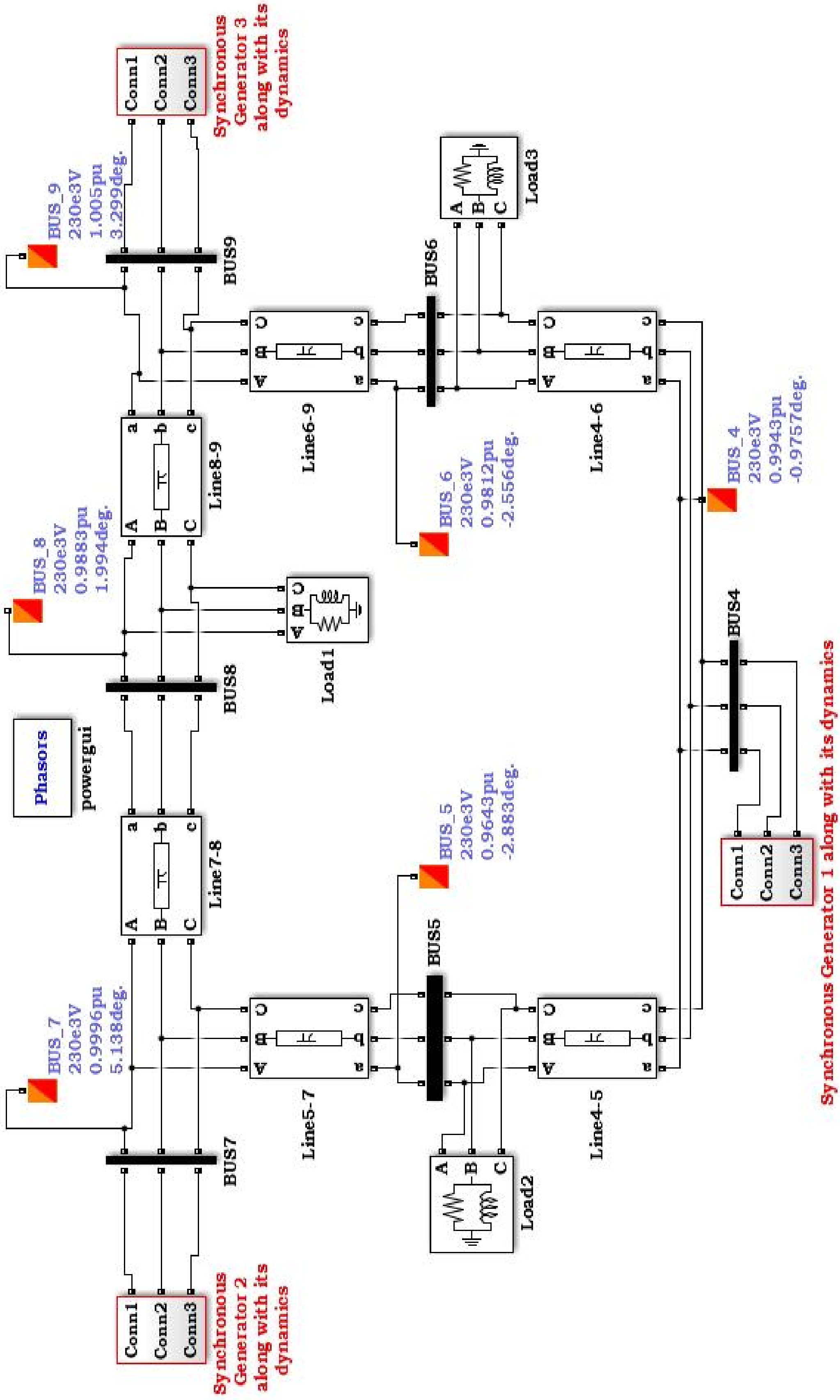

Figure 3.1: WSCC 3-generator, 9-bus system

Table 3.1: Generator Data

Generator	**1**	**2**	**3**
Rated MVA	247.5	192.0	128.0
kV	16.5	18.0	13.8
Power Factor	1.0	0.85	0.85
Type	hydro	steam	steam
Speed	180r/min	3600r/min	3600r/min
x_d	0.1460	0.8958	1.3125
x'_d	0.0608	0.1198	0.1813
x_q	0.0969	0.8645	1.2578
x'_q	0.0969	0.1969	0.25
x_l(leakage)	0.0336	0.0521	0.0742
T'_{do}	8.96	6.00	5.89
T'_{qo}	0	0.535	0.600

Table 3.2: Load Data

Load connected to bus	**P(MW)**	**Q(MW)**
5	125	50
6	90	30
8	100	35

By using the data given in tables 3.1, 3.2, 3.3 and 3.4, the model shown in Fig.3.1 has been simulated in MATLAB®. As seen in the Fig.3.1 , there are 9 buses in the system from which 6 buses can be observed and the other 3 buses are part of the subsystems shown in figures 3.2, 3.3 and 3.4.

The subsystems seen include the synchronous generators along with their governor and exciter systems. Loads 1, 2 and 3 are the inductive loads connected to the system. The orange colour tool indicates the load flow tool required for indicating the voltage magnitudes and phase angles at each buses.

The simulation is carried out to know the active and reactive power of the three machines along with the voltage magnitudes and phase angles at each bus.

The data to be inserted in the governor and excitation systems is given in the table

Table 3.3: Transmission Line Data per Km

Line Between Buses	**R(Ω)**	**L(H)** $*\mathbf{e}^{-3}$	**C(F)** $*\mathbf{e}^{-4}$
7-8	0.0085	0.1909	1.976
8-9	0.0119	0.2673	2.7719
5-7	0.032	0.427	4.058
6-9	0.039	0.4509	4.748
4-5	0.010	0.2254	2.334
4-6	0.017	0.244	2.0955

Table 3.4: Exciter Data

Parameters	**Exciter** 1	**Exciter** 2	**Exciter** 3
K_A	20	20	20
T_A(sec)	0.2	0.2	0.2
K_E	1.0	1.0	1.0
T_E(sec)	0.314	0.314	0.314
K_F	0.063	0.063	0.063
T_F(sec)	0.35	0.35	0.35

3.4. The subsystems shown in figures 3.2, 3.3 and 3.4 include the exciter and governor systems for the generator 1, 2 and 3.

Synchronous Generator 1 is a hydro generator. So, accordingly the type of governor used for this machine will be of hydro type. Being a hydro generator, this machine is a salient-pole machine and will have the lowest speed as the number of poles for this machine are more as compared to other two machines. This subsytem is shown in Fig. 3.2.

Synchronous Generator 2 and Generator 3 are steam generators. So, accordingly the type of governor used for this machine will be of steam type. Being a steam generator, these machines will be of cylindrical type and will have a greater speed as the number of poles for this machine are less as compared to machine 1. These subsystems are shown in Fig. 3.3 and 3.4 respectively.

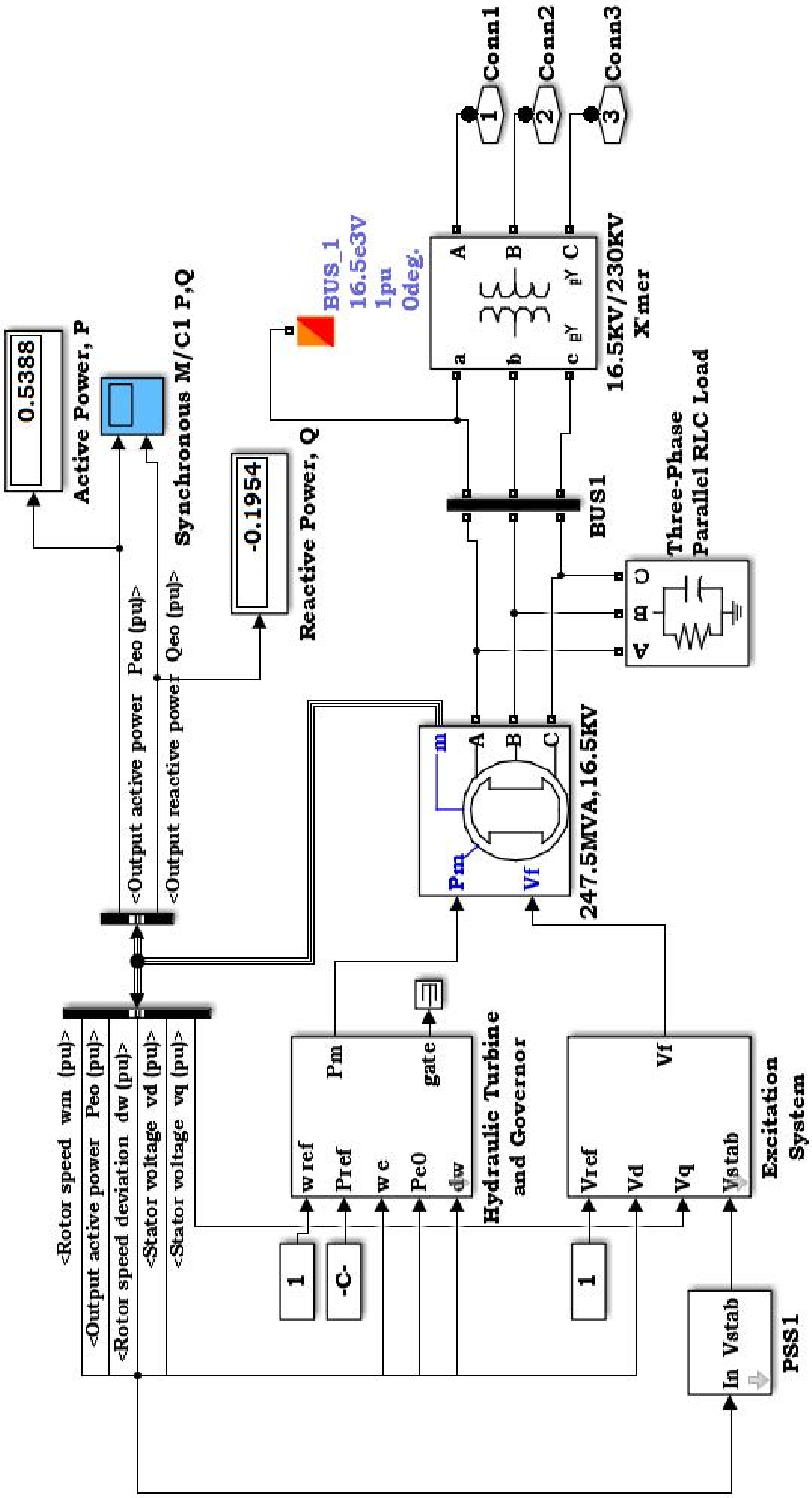

Figure 3.2: Subsystem showing Governor and Excitation System For Synchronous Generator 1

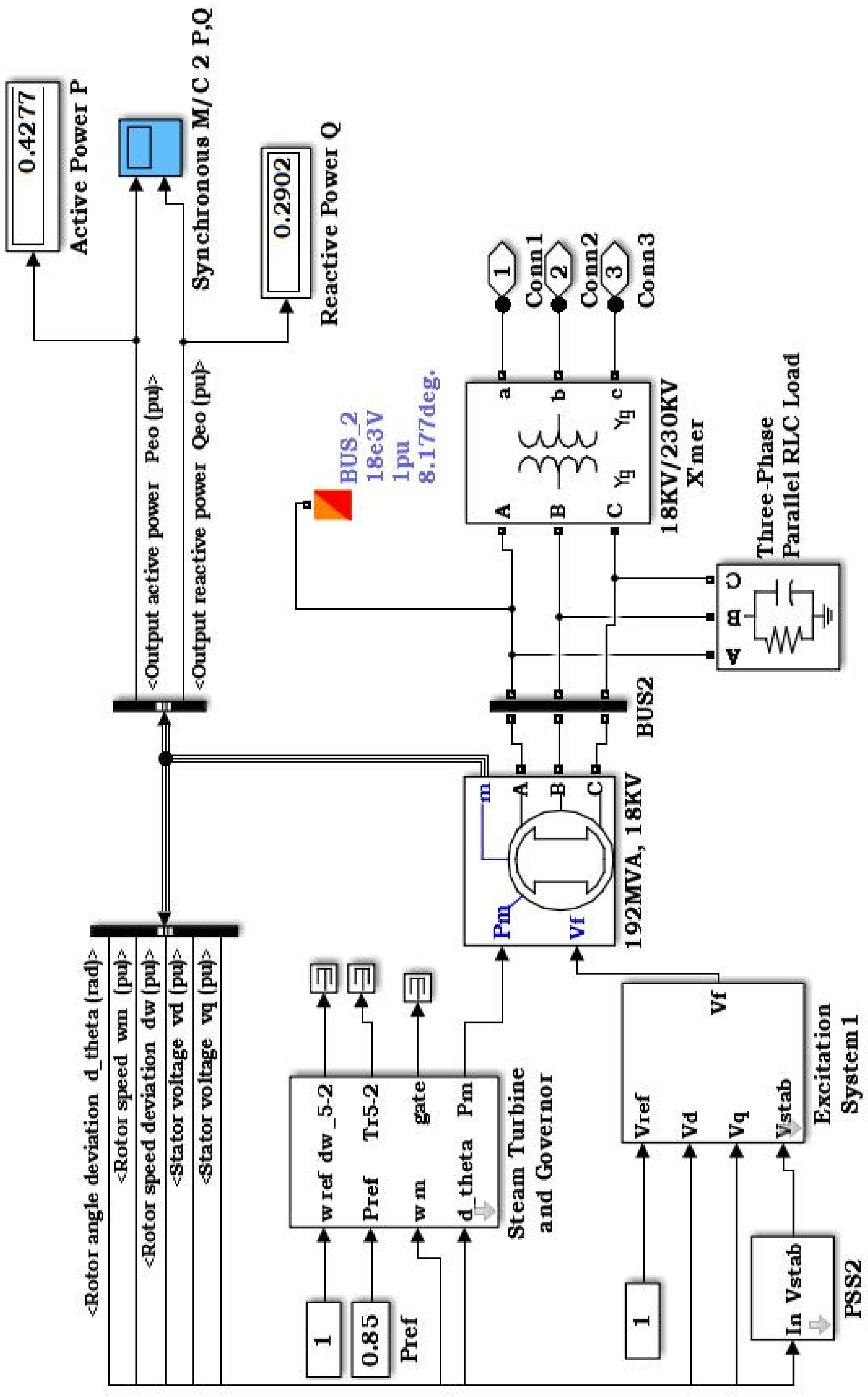

Figure 3.3: Subsystem showing Governor and Excitation System For Synchronous Generator 2

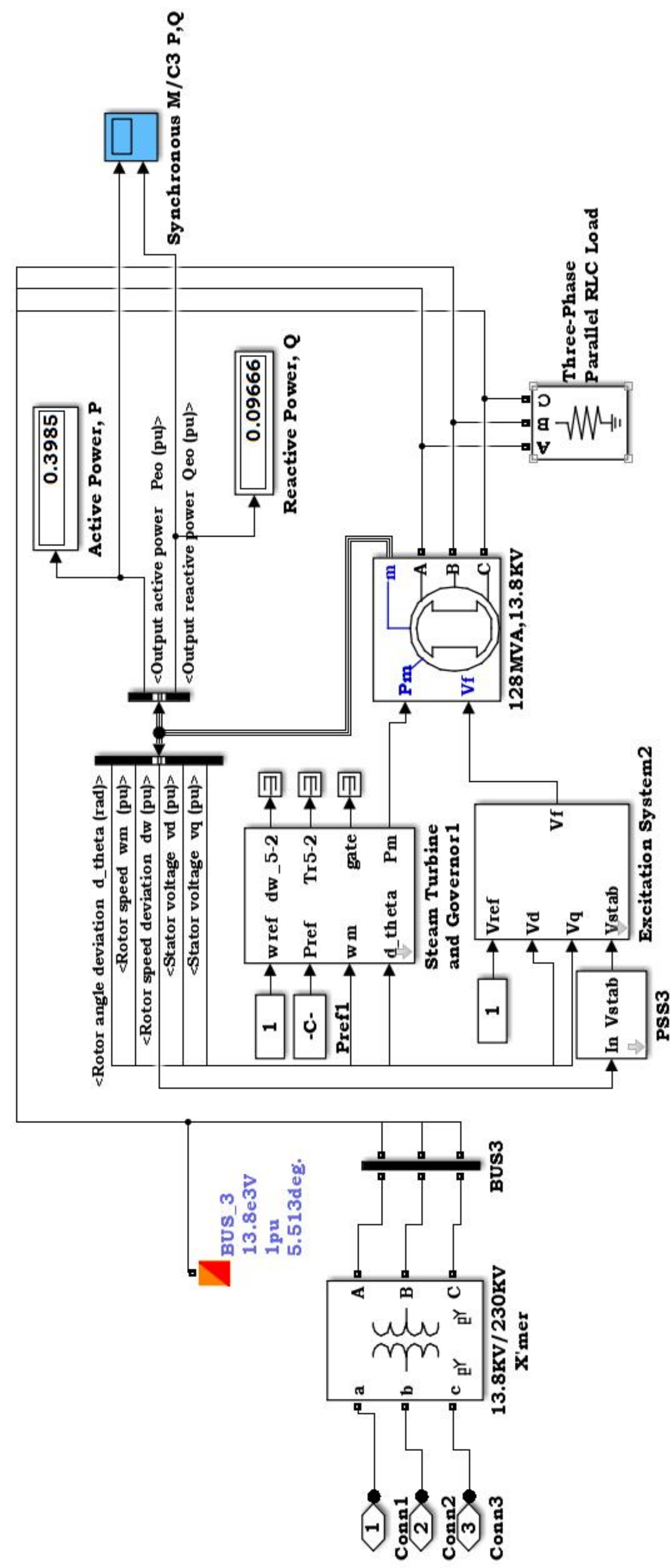

Figure 3.4: Subsystem showing Governor and Excitation System For Synchronous Generator 3

3.1.2 Results and Analysis

First step is to carry out the steady state analysis of the system. This means static analysis has to be done in which the active power, reactive power and voltage magnitudes at each bus have to be calculated. As it is steady state analysis,the machines should reach steady state after a small interval of time. This is indicated by a straight line in the graphs of active and reactive power for each machine as shown below. The load flow tool is used which indicated the bus voltage magnitudes and phase angles at each buses once the load flow converges for the system.

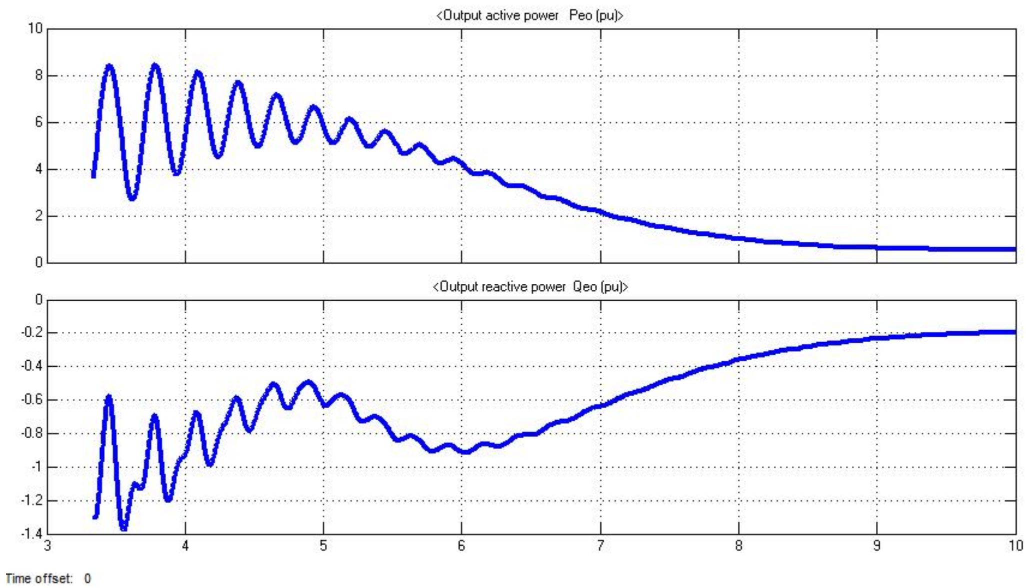

Figure 3.5: Simulation result of Synchronous Generator 1 Active and Reactive Power

From the above figure,it can be seen that machine 1 has stabilized at an active power of 0.5384pu and reactive power of -0.1954pu.

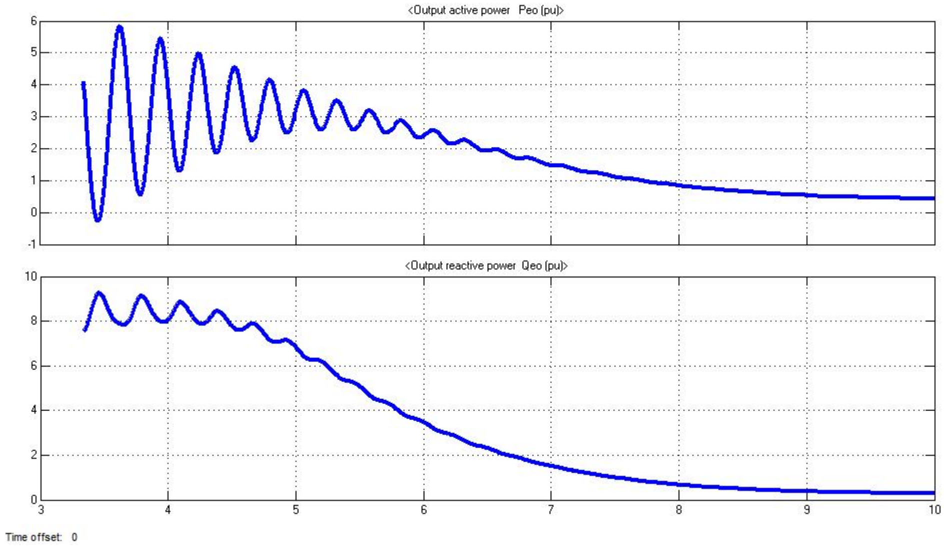

Figure 3.6: Simulation result of Synchronous Generator 2 Active and Reactive Power

From the above figure,it can be seen that machine 2 has stabilized at an active power of 0.4279pu and reactive power of 0.2901pu.

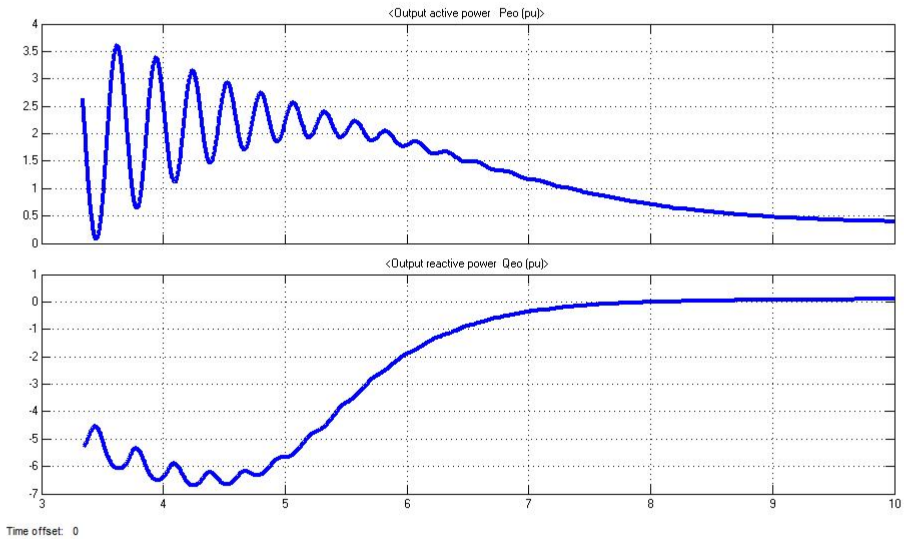

Figure 3.7: Simulation result of Synchronous Generator 3 Active and Reactive Power

From the above figure,it can be seen that machine 3 has stabilized at an active power of 0.3986pu and reactive power of 0.09663pu.

3.1.3 Load Flow Analysis of The System

The load flow analysis of any system is carried out to know the steady state behaviour of the system. The load flow is computed at 100 MVA base and 60 Hz frequency. Number of iterations needed to compute this load flow is 2. The load tool uses the Newton-Raphson method to provide a robust and fast convergence solution.

The analysis report is as follows:

Total generation : P = 320.94 MW, Q = 21.31 Mvar

Total PQ load : P = 315.00 MW, Q = 115.00 Mvar

Total Zshunt load : P = 1.13 MW, Q = -0.56 Mvar

Total ASM load : P = 0.00 MW, Q = 0.00 Mvar

Total losses : P = 4.81 MW, Q = -93.13 Mvar

a. **BUS 1: V = 1.000 pu/16.5kV, 0.00 deg ; Swing bus**
   Generation : P = 72.94 MW, Q = 24.66 Mvar
   $PQ_l oad$: P = 0.00 MW, Q = 0.00 Mvar
   $Z_s hunt$: P = 0.00 MW, Q = -0.50 Mvar
   BUS4 : P = 72.94 MW, Q = 25.16 Mvar

b. **BUS 2: V = 1.000 pu/18kV, 8.15 deg**
   Generation : P = 163.00 MW, Q = 4.77 Mvar
   PQ_{load} : P = 0.00 MW, Q = 0.00 Mvar
   Z_{shunt} : P = 0.38 MW, Q = -0.81 Mvar
   BUS 7 : P = 162.62 MW, Q = 5.58 Mvar

c. **BUS 3: V = 1.000 pu/13.8kV, 5.50 deg**

Generation : P = 85.00 MW, Q = -8.13 Mvar

PQ_{load} : P = 0.00 MW, Q = 0.00 Mvar

Z_{shunt} : P = 0.26 MW, Q = 0.26 Mvar

BUS 9 : P = 84.74 MW, Q = -8.39 Mvar

d. **BUS 4: V = 0.994 pu/230kV, -0.98 deg**

Generation : P = 0.00 MW, Q = 0.00 Mvar

PQ_{load} : P = 0.00 MW, Q = -0.00 Mvar

Z_{shunt} : P = 0.49 MW, Q = 0.49 Mvar

BUS 1 : P = -72.94 MW, Q = -23.78 Mvar

BUS 5 : P = 41.41 MW, Q = 22.23 Mvar

BUS 6 : P = 31.04 MW, Q = 1.06 Mvar

e. **BUS 5: V = 0.964 pu/230kV, -2.89 deg**

Generation : P = 0.00 MW, Q = 0.00 Mvar

PQ_{load} : P = 125.00 MW, Q = 50.00 Mvar

Z_{shunt} : P = 0.00 MW, Q = -0.00 Mvar

BUS 4 : P = -41.14 MW, Q = -36.84 Mvar

BUS 7 : P = -83.86 MW, Q = -13.16 Mvar

f. **BUS 6: V = 0.981 pu/230kV, -2.56 deg**

Generation : P = 0.00 MW, Q = 0.00 Mvar

PQ_{load} : P = 90.00 MW, Q = 30.00 Mvar

Z_{shunt} : P = 0.00 MW, Q = -0.00 Mvar

BUS 4 : P = -30.86 MW, Q = -15.52 Mvar

BUS 9 : P = -59.14 MW, Q = -14.48 Mvar

g. **BUS 7: V = 1.000 pu/230kV, 5.12 deg**
   Generation : P = 0.00 MW, Q = 0.00 Mvar
   PQ_{load} : P = 0.00 MW, Q = -0.00 Mvar
   Z_{shunt} : P = -0.00 MW, Q = 0.00 Mvar
   BUS 2 : P = -162.62 MW, Q = 3.04 Mvar
   BUS 5 : P = 86.24 MW, Q = -4.38 Mvar
   BUS 8 : P = 76.38 MW, Q = 1.35 Mvar

h. **BUS 8: V = 0.988 pu/230kV, 1.98 deg**
   Generation : P = 0.00 MW, Q = 0.00 Mvar
   PQ_{load} : P = 100.00 MW, Q = 35.00 Mvar
   Z_{shunt} : P = -0.00 MW, Q = -0.00 Mvar
   BUS 7 : P = -75.88 MW, Q = -11.83 Mvar
   BUS 9 : P = -24.12 MW, Q = -23.17 Mvar

i. **BUS 9: V = 1.005 pu/230kV, 3.29 deg**
   Generation : P = 0.00 MW, Q = 0.00 Mvar
   PQ_{load} : P = 0.00 MW, Q = -0.00 Mvar
   Z_{shunt} : P = -0.00 MW, Q = -0.00 Mvar
   BUS 9 : P = -84.74 MW, Q = 11.71 Mvar
   BUS 6 : P = 60.53 MW, Q = -14.88 Mvar
   BUS 8 : P = 24.22 MW, Q = 3.17 Mvar

It can be seen that the bus power and voltages closely matches the load flow given in reference [10]. This indicates that the model is perfectly working. This is indicated in **bold** in the above analysis.

Thus, a comparison can be made for the actual and simulated results on the basis of the load flow analysis carried out. The actual bus voltage magnitudes and phase angles and those obtained in simulation have been presented in the below tables.

Table 3.5: Voltage at each Bus in pu

Bus Number	**Actual**	**Simulated**
1	1.04	1
2	1.025	1
3	1.025	1
4	1.026	0.9943
5	0.996	0.9643
6	1.013	0.9812
7	1.026	0.9996
8	1.016	0.9883
9	1.032	1.0046

Table 3.6: Phase Angles at each Bus in degree

Bus Number	**Actual**	**Simulated**
1	0	0
2	9.3	0.02168
3	4.7	8.15
4	-2.2	-0.98
5	-4	-2.89
6	-3.7	-2.56
7	3.7	5.12
8	0.7	1.98
9	2.0	3.29

3.1.4 System Modeling for WSCC 3-Generator, 9-Bus System

The two-axis classical synchronous generator model of the system is considered. Assumptions for thee modeling are:

- Subtransient reactances and saturation are neglected.
- The turbine governor dynamics are neglected resulting in mechanical power P_{Mi} being constant.

So, the resulting differential-algebraic equations for the system can be written in matrix form as:

$$\begin{bmatrix} \dot{E}'_{qi} \\ \dot{E}'_{di} \\ \dot{\delta}_i \\ \dot{\omega}_i \\ \dot{E}_{fdi} \\ \dot{R}_{fi} \\ \dot{V}_{Ri} \end{bmatrix} = \begin{bmatrix} A_i \end{bmatrix} \begin{bmatrix} E'_{qi} \\ E'_{di} \\ \delta_i \\ \omega_i \\ E_{fdi} \\ R_{fi} \\ V_{Ri} \end{bmatrix} + R_i \left(E'_{qi}, \quad E'_{di}, \quad E_{fdi}, \quad I_{di}, \quad I_{qi}, \quad V_i \right) + C_i u_i \tag{3.1}$$

i=1,2,3 where

E'_{qi} = transient EMF in the quadrature axis of the i^{th} generator in p.u.
E'_{di} = transient EMF in the direct axis of the i^{th} generator in p.u.
δ_i = rotor angle of the i^{th} generator
ω_i = relative speed of the i^{th} generator
E_{fdi} = field voltage in the direct axis of the i^{th} generator in p.u.
I_{di} = direct axis current of the i^{th} generator in p.u.
I_{qi} = quadrature axis current of the i^{th} generator in p.u.
V_i = voltage of the i^{th} generator in p.u.
A_i = system matrix of the i^{th} generator

The state matrix for the i^{th} generator of the system is given by:

$$A_i = \begin{bmatrix} \frac{-1}{T'_{doi}} & 0 & 0 & 0 & \frac{1}{T'_{doi}} & 0 & 0 \\ 0 & \frac{-1}{T'_{qoi}} & 0 & 0 & 0 & 0 & 0 \\ 0 & 0 & 0 & 1 & 0 & 0 & 0 \\ 0 & 0 & 0 & \frac{-D_i}{M_i} & 0 & 0 & 0 \\ 0 & 0 & 0 & 0 & \frac{-K_{Ei}}{T_{Ei}} & 0 & \frac{1}{T_{Ei}} \\ 0 & 0 & 0 & 0 & \frac{K_{Fi}}{T_F^2} & \frac{-1}{T_{Fi}} & 0 \\ 0 & 0 & 0 & 0 & \frac{-K_{Ai}K_{Fi}}{T_{Ai}T_{Fi}} & \frac{K_{Ai}}{T_{Ai}} & \frac{-1}{T_{Ai}} \end{bmatrix} \tag{3.2}$$

i=1,2,3 where,

T'_{doi} = direct axis transient short circuit time constant in seconds

T'_{qoi} = quadrature axis transient short circuit time constant in seconds

K_{Ei} = exciter gain of the i^{th} generator

T_{Ei} = exciter time constant of the i^{th} generator

K_{Ai} = regulator gain of exciter of the i^{th} generator

T_{Ai} = regulator time constant of exciter of the i^{th} generator

K_{Fi} = damping filter gain of exciter of the i^{th} generator

T_{Fi} = damping filter time constant of exciter of the i^{th} generator

Using equation 3.2, the state matrices for the three generators can be computed.

For generator 1,

$T'_{do1} = 8.96$ secs, $T'_{qo1} = 0.31$ sec, $\frac{D_1}{M_1} = 0.1$, $K_{E1} = 1.0$, $T_{E1} = 0.314$, $K_{A1} = 20$, $T_{A1} = 0.2$, $K_{F1} = 0.063$, $T_{F1} = 0.35$

Using the above information, the state matrix for generator 1 is given by :

$$A_1 = \begin{bmatrix} -0.1116 & 0 & 0 & 0 & 0.1116 & 0 & 0 \\ 0 & -3.225 & 0 & 0 & 0 & 0 & 0 \\ 0 & 0 & 0 & 1 & 0 & 0 & 0 \\ 0 & 0 & 0 & -0.1 & 0 & 0 & 0 \\ 0 & 0 & 0 & 0 & -3.184 & 0 & 3.184 \\ 0 & 0 & 0 & 0 & 0.514 & -2.857 & 0 \\ 0 & 0 & 0 & 0 & -18 & 100 & -5 \end{bmatrix} \tag{3.3}$$

For generator 2,

$T'_{do2} = 6$ secs, $T'_{qo2} = 0.535$ secs, $\frac{D_2}{M_2} = 0.2$, $K_{E2} = 1.0$, $T_{E2} = 0.314$, $K_{A2} = 20$, $T_{A2} = 0.2$, $K_{F2} = 0.063$, $T_{F2} = 0.35$

Using the above information, the state matrix for generator 2 is given by :

$$A_2 = \begin{bmatrix} -0.166 & 0 & 0 & 0 & 0.166 & 0 & 0 \\ 0 & -1.869 & 0 & 0 & 0 & 0 & 0 \\ 0 & 0 & 0 & 1 & 0 & 0 & 0 \\ 0 & 0 & 0 & -0.2 & 0 & 0 & 0 \\ 0 & 0 & 0 & 0 & -3.184 & 0 & 3.184 \\ 0 & 0 & 0 & 0 & 0.514 & -2.857 & 0 \\ 0 & 0 & 0 & 0 & -18 & 100 & -5 \end{bmatrix} \tag{3.4}$$

For generator 3,

$T'_{do3} = 5.89$ secs, $T'_{qo3} = 0.6$ secs, $\frac{D_3}{M_3} = 0.3$, $K_{E3} = 1.0$ $T_{E3} = 0.314$, $K_{A3} = 20$, $T_{A3} = 0.2$, $K_{F3} = 0.063$, $T_{F3} = 0.35$

Using the above information, the state matrix for generator 3 is given by :

$$A_3 = \begin{bmatrix} -0.169 & 0 & 0 & 0 & 0.169 & 0 & 0 \\ 0 & -1.666 & 0 & 0 & 0 & 0 & 0 \\ 0 & 0 & 0 & 1 & 0 & 0 & 0 \\ 0 & 0 & 0 & -0.3 & 0 & 0 & 0 \\ 0 & 0 & 0 & 0 & -3.184 & 0 & 3.184 \\ 0 & 0 & 0 & 0 & 0.514 & -2.857 & 0 \\ 0 & 0 & 0 & 0 & -18 & 100 & -5 \end{bmatrix} \tag{3.5}$$

Thus, the entire system state matrix A can be written as:

$$A = \begin{bmatrix} A_1 & 0 & 0 \\ 0 & A_2 & 0 \\ 0 & 0 & A_3 \end{bmatrix} \tag{3.6}$$

The above matrix will be of the order (21 $\times$ 21).

3.2 Renewable Energy Management System

After obtaining the steady state results, the next objective is to replace one of the synchronous generator by a renewable source.

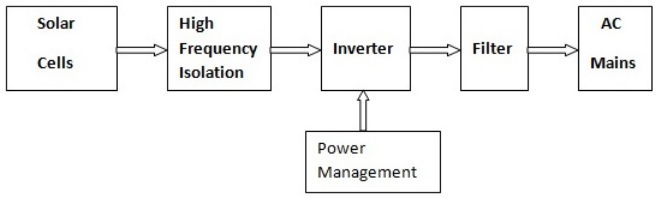

Figure 3.8: Block Diagram indicating a Renewable Power System for connecting directly to the ac mains

The above figure 3.8 represents a block diagram of a renewable energy-management system. The renewable energy source (in this case solar cells) is directly connected to the main grid. The direction of flow of power has to be from the renewable source to the ac mains. The power factor of the main grid and controlling of the dc voltage of the renewable energy source is done by the invertor. The power management system is responsible for controlling of the dc voltage so as to maximize the power extracted from the renewable energy source(solar cells)[13].

The Fig. 3.10 shows the connection to the ac mains to a generic renewable energy. The renewable energy source i.e. solar in this case is represented as a current source which is attached to the dc side of the inverter. Through an inductive filter, the inverter is connected to the main grid. Thus, the entire network is assumed to be a constant dc voltage source. This system is used to replace the synchronous generator which was present at bus 3 in the conventional WSCC 3-generator 9-bus system. So, this system is desired to generate 85 MW power.
Fig. 3.9 shows how a renewable source is integrated with the conventional WSCC 3-generator, 9-bus system. Fig. 3.10 shows the subsystem which consists of the renewable energy management system. The figure has been properly labelled so that system modeling can be easily understood which has been explained in the later part of this chapter.

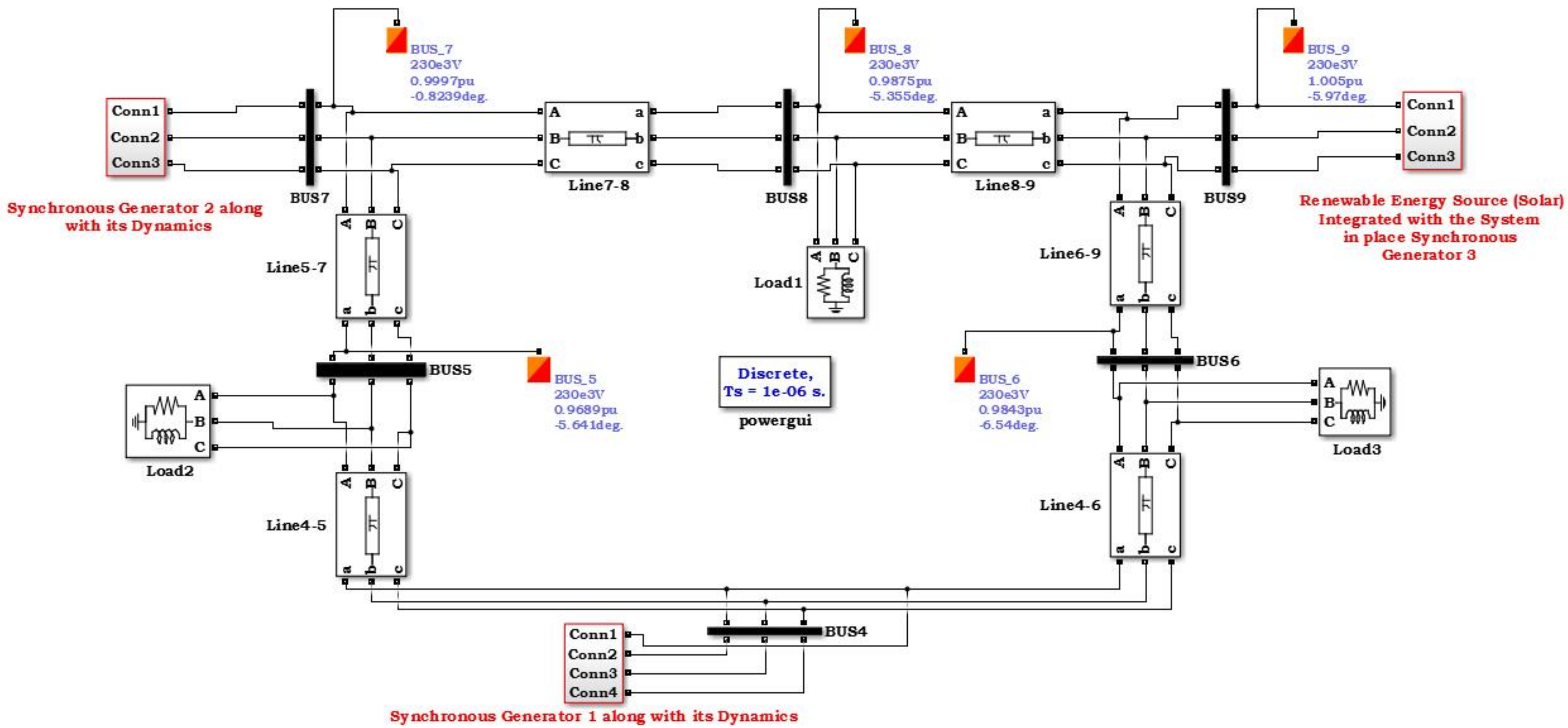

Figure 3.9: Integration of Renewable Source(Solar) into the system in place of synchronous generator of 85 MW

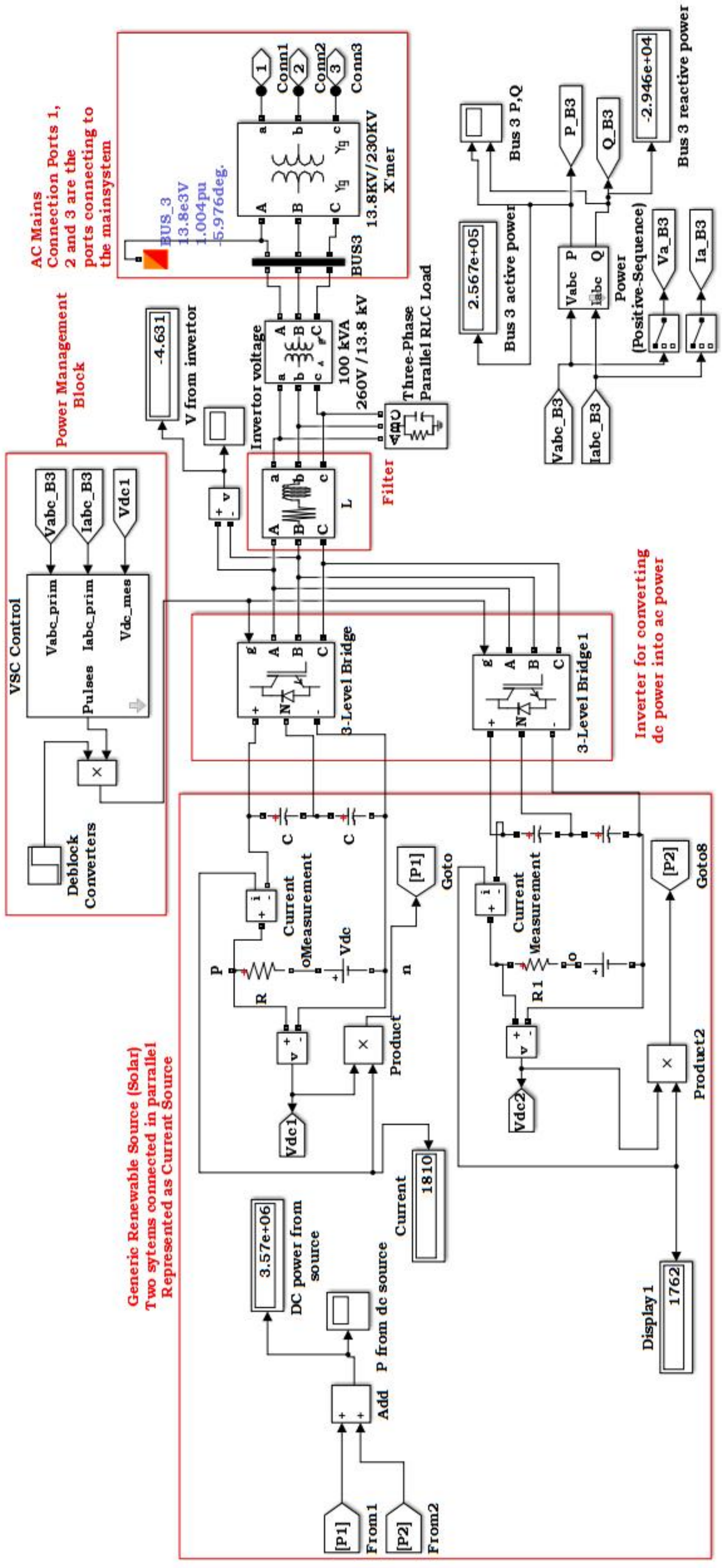

Figure 3.10: Subsystem showing the Renewable(Solar) Energy Management System

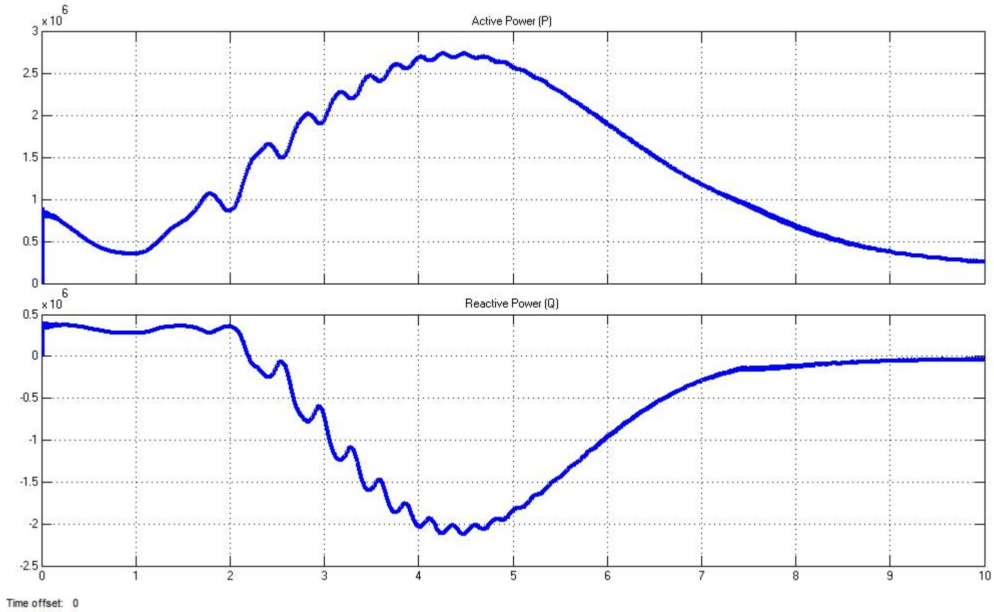

Figure 3.11: Output active and reactive power

In the above figure, the power waveforms are becoming straight after a time interval i.e. 8 secs indicating system to be in stable region. However, the power results obtained is not as expected.

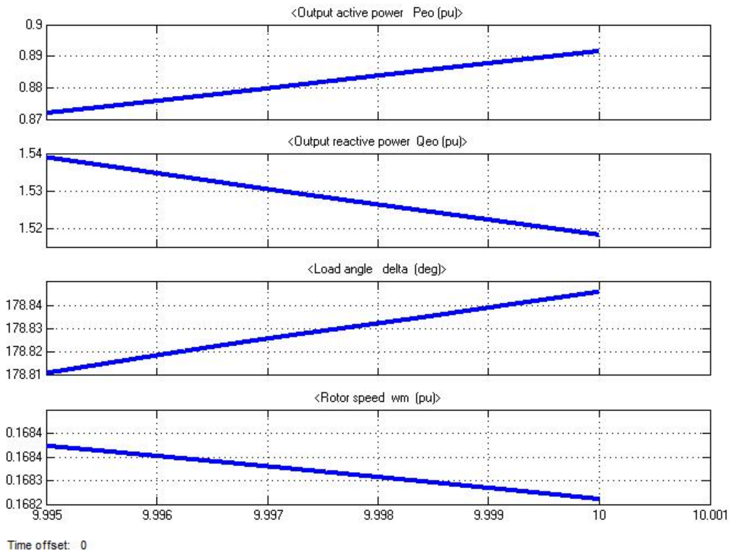

Figure 3.12: Effects on active power, reactive power, load angle and speed of rotor of Synchronous generator 1 after integrating solar at bus 3

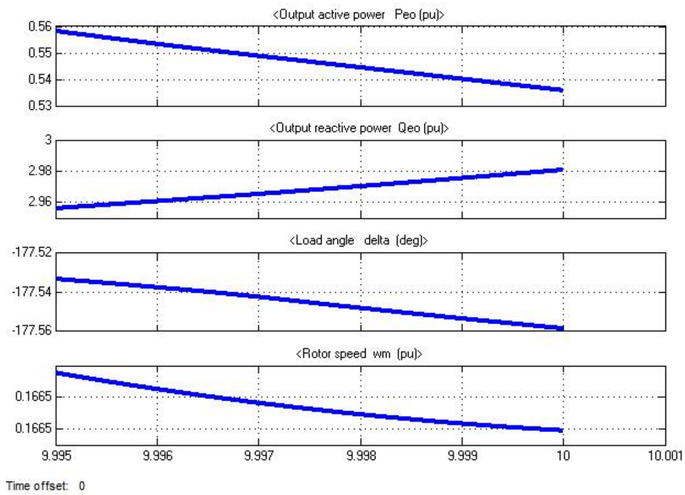

Figure 3.13: Effects on active power, reactive power, load angle and speed of rotor of Synchronous generator 2 after integrating solar at bus 3

From the above figures, it can be seen that there is significant difference in the results as compared to the results of the conventional system indicated in Fig. 3.5, 3.7 and 3.6 when a renewable energy source is integrated into the system. The results of the system integration could not lead to any meaningful conclusion of system's behaviour.

3.2.1 System Modeling when the Synchronous Generator 3 is replaced by Renewable Energy Source

The four state variables considered for the Solar system are:

- voltage of the dc link, denoted by v_{pn}
- voltage balance of the dc-link , denoted by v_o
- Two line currents (inductor currents), denoted by i_{yd} and i_{yq} in d-q domain.

Here, the model is assumed to have a relatively high switching frequency and no losses.

Considering the above state variables, the system can be represented in matrix form as:

$$\begin{bmatrix} \dot{i}_{yd} \\ \dot{i}_{yq} \\ \dot{v}_{pn} \\ \dot{v}_o \end{bmatrix} = \begin{bmatrix} 0 & \omega_r & \frac{d_{pd}-d_{nd}}{2L} & \frac{d_{pd}+d_{nd}}{2L} \\ -\omega_r & 0 & \frac{d_{pq}-d_{nq}}{2L} & \frac{d_{pq}+d_{nq}}{2L} \\ \frac{d_{pd}+d_{nd}}{C} & \frac{d_{pq}+d_{nq}}{C} & 0 & 0 \\ \frac{-d_{pd}-d_{nd}}{C} & \frac{-d_{pq}-d_{nq}}{C} & 0 & 0 \end{bmatrix} \begin{bmatrix} i_{yd} \\ i_{yq} \\ v_{pn} \\ v_o \end{bmatrix} + \begin{bmatrix} \frac{-1}{L} & 0 & 0 \\ 0 & \frac{-1}{L} & 0 \\ 0 & 0 & \frac{2}{C} \\ 0 & 0 & 0 \end{bmatrix} \begin{bmatrix} v_{yd} \\ v_{yq} \\ i_{dc} \end{bmatrix} \quad (3.7)$$

where

v_{pn} = dc link voltage

v_o = dc link voltage balance

v_{yd} = d-axis components of line to neutral voltages of the three phases

v_{yq} = q-axis components of line to neutral voltages of the three phases

i_{yd} = d-axis components of currents of the three phases

i_{yq} = q-axis components of currents of the three phases

d_{pd} = d-axis components of d_{ap}, d_{bp}, d_{cp}

d_{pq} = q-axis components of d_{ap}, d_{bp}, d_{cp}

d_{nd} = d-axis components of d_{an}, d_{bn}, d_{cn}

d_{nq} = q-axis components of d_{an}, d_{bn}, d_{cn}

Here, d_{pd}, d_{pq}, d_{nd} and d_{nq} are the control variables and as the state matrix comprises of these variables, the state space model obtained in equation 3.7 is nonlinear and is applicable to large-signal operation. Thus, linearization of the model is required

around the operating points which results in a small-signal model. In order to implement an integral control of the state variables $\hat{i}_{yq}$, $\hat{v}_{pn}$ and $\hat{v}_o$, three additional state variables have to be incorporated in the system which are I$\hat{i}_{yq}$, I$\hat{v}_{pn}$ and I$\hat{v}_o$.
Thus, linearizing the state space model in equation 3.7 yields :

$$\begin{bmatrix} \dot{\hat{i}}_{yd} \\ \dot{\hat{i}}_{yq} \\ \dot{\hat{v}}_{pn} \\ \dot{\hat{v}}_{o} \\ \dot{I\hat{i}}_{yq} \\ \dot{I\hat{v}}_{pn} \\ \dot{I\hat{v}}_{o} \end{bmatrix} = \begin{bmatrix} 0 & \omega_r & \frac{D_{pd}-D_{nd}}{2L} & \frac{D_{pd}+D_{nd}}{2L} & 0 & 0 & 0 \\ -\omega_r & 0 & \frac{D_{pq}-D_{nq}}{2L} & \frac{D_{pq}+D_{nq}}{2L} & 0 & 0 & 0 \\ \frac{D_{pd}+D_{nd}}{C} & \frac{D_{pq}+D_{nq}}{C} & 0 & 0 & 0 & 0 & 0 \\ \frac{-D_{pd}-D_{nd}}{C} & \frac{-D_{pq}-D_{nq}}{C} & 0 & 0 & 0 & 0 & 0 \\ 0 & 1 & 0 & 0 & 0 & 0 & 0 \\ 0 & 0 & 1 & 0 & 0 & 0 & 0 \\ 0 & 0 & 0 & 1 & 0 & 0 & 0 \end{bmatrix} \begin{bmatrix} \hat{i}_{yd} \\ \hat{i}_{yq} \\ \hat{v}_{pn} \\ \hat{v}_{o} \\ I\hat{i}_{yq} \\ I\hat{v}_{pn} \\ I\hat{v}_{o} \end{bmatrix}$$
$$+ \begin{bmatrix} \frac{V_{pn}+V_o}{2L} & \frac{V_o-V_{pn}}{2L} & 0 & 0 \\ 0 & 0 & \frac{V_{pn}+V_o}{2L} & \frac{V_o-V_{pn}}{2L} \\ \frac{-I_{yd}}{C} & \frac{I_{yd}}{C} & \frac{-I_{yq}}{C} & \frac{I_{yq}}{C} \\ \frac{-I_{yd}}{C} & \frac{-I_{yd}}{C} & \frac{-I_{yq}}{C} & \frac{-I_{yq}}{C} \\ 0 & 0 & 0 & 0 \\ 0 & 0 & 0 & 0 \\ 0 & 0 & 0 & 0 \end{bmatrix} \begin{bmatrix} \hat{d}_{pd} \\ \hat{d}_{nd} \\ \hat{d}_{pq} \\ \hat{d}_{nd} \end{bmatrix} + \begin{bmatrix} \frac{-1}{L} & 0 & 0 \\ 0 & \frac{-1}{L} & 0 \\ 0 & 0 & \frac{2}{C} \\ 0 & 0 & 0 \\ 0 & 0 & 0 \\ 0 & 0 & 0 \\ 0 & 0 & 0 \end{bmatrix} \begin{bmatrix} \hat{v}_{yd} \\ \hat{v}_{yq} \\ \hat{i}_{dc} \end{bmatrix} \tag{3.8}$$

where

$$D_{pd} = D_{nd} = \frac{V_{yd}}{V_{pn}} - \frac{\omega_r \times L \times I_{dc} \times V_{yq}}{V_{yd}^2 + V_{yq}^2} \tag{3.9}$$

$$D_{pq} = D_{nq} = \frac{V_{yq}}{V_{pn}} - \frac{\omega_r \times L \times I_{dc} \times V_{yd}}{V_{yd}^2 + V_{yq}^2} \tag{3.10}$$

$$I_{yd} = \frac{V_{pn} \times I_{dc} \times V_{yd}}{V_{yd}^2 + V_{yq}^2} \tag{3.11}$$

$$I_{yq} = \frac{V_{pn} \times I_{dc} \times V_{yq}}{V_{yd}^2 + V_{yq}^2} \tag{3.12}$$

$$V_o = 0 \tag{3.13}$$

From the simulations performed, the results obtained for the various parameters are as follows: $V_{yd} = 1.133$ V, $V_{pn} = 1000$ V, $\omega_r = 1.66\ H_z$, L $= 250e^{-6}$ H, $I_{dc} = 1762$ A, $V_{yq} = -0.00396$ V, C $= 10000e^{-6}$ F, $V_o = 0$.

Thus, substituting the above obtained results in equations 3.9, 3.10, 3.11, 3.12 and 3.13, the following results are obtained: $D_{pd} = D_{nd} = 5.592$, $D_{pq} = D_{nq} = 1599.749$, $I_{yd} = 1555.144$ kA, $I_{yq} =$ -5435.455 A.

Finally, substituting the above calculated results in 3.9, the state space model for the solar system is given by:

$$\begin{bmatrix} \dot{\hat{i}}_{yd} \\ \dot{\hat{i}}_{yq} \\ \dot{\hat{v}}_{pn} \\ \dot{\hat{v}}_{o} \\ \dot{I}\hat{i}_{yq} \\ \dot{I}\hat{v}_{pn} \\ \dot{I}\hat{v}_{o} \end{bmatrix} = \begin{bmatrix} 0 & 1.66 & 0 & 9.023 & 0 & 0 & 0 \\ -1.66 & 0 & 0 & 2581.539 & 0 & 0 & 0 \\ 0.451 & 129.076 & 0 & 0 & 0 & 0 & 0 \\ -0.451 & -129.076 & 0 & 0 & 0 & 0 & 0 \\ 0 & 1 & 0 & 0 & 0 & 0 & 0 \\ 0 & 0 & 1 & 0 & 0 & 0 & 0 \\ 0 & 0 & 0 & 1 & 0 & 0 & 0 \end{bmatrix} \begin{bmatrix} \hat{i}_{yd} \\ \hat{i}_{yq} \\ \hat{v}_{pn} \\ \hat{v}_{o} \\ I\hat{i}_{yq} \\ I\hat{v}_{pn} \\ I\hat{v}_{o} \end{bmatrix} \tag{3.14}$$

$$+10^3 \begin{bmatrix} 0.806 & -0.806 & 0 & 0 \\ 0 & 0 & 20 & -0.806 \\ -62.738 & 62.738 & 0.219 & -0.219 \\ -62.738 & -62.738 & 0.219 & 0.219 \\ 0 & 0 & 0 & 0 \\ 0 & 0 & 0 & 0 \\ 0 & 0 & 0 & 0 \end{bmatrix} \begin{bmatrix} \hat{d}_{pd} \\ \hat{d}_{nd} \\ \hat{d}_{pq} \\ \hat{d}_{nd} \end{bmatrix} + \begin{bmatrix} -1.613 & 0 & 0 \\ 0 & -1.613 & 0 \\ 0 & 0 & 0.08 \\ 0 & 0 & 0 \\ 0 & 0 & 0 \\ 0 & 0 & 0 \\ 0 & 0 & 0 \end{bmatrix} \begin{bmatrix} \hat{v}_{yd} \\ \hat{v}_{yq} \\ \hat{i}_{dc} \end{bmatrix}$$

where the state matrix A_3 when solar system is integrated into the WSCC 3 machine 9 bus system at bus 3 is given by :

$$A_{31} = \begin{bmatrix} 0 & 1.66 & 0 & 9.023 & 0 & 0 & 0 \\ -1.66 & 0 & 0 & 2581.539 & 0 & 0 & 0 \\ 0.451 & 129.076 & 0 & 0 & 0 & 0 & 0 \\ -0.451 & -129.076 & 0 & 0 & 0 & 0 & 0 \\ 0 & 1 & 0 & 0 & 0 & 0 & 0 \\ 0 & 0 & 1 & 0 & 0 & 0 & 0 \\ 0 & 0 & 0 & 1 & 0 & 0 & 0 \end{bmatrix} \tag{3.15}$$

Thus, when a renewable energy source (solar) is integrated into the system, in the entire system matrix represented in equation 3.6, the matrix A_3 given in equation 3.5 will be replaced by the matrix A_{31} given in equation 3.15 as

$$A = \begin{bmatrix} A_1 & 0 & 0 \\ 0 & A_2 & 0 \\ 0 & 0 & A_{31} \end{bmatrix} \tag{3.16}$$

The above matrix will also be of the order (21×21).

3.3 Addition of Noise to the Captured Measurements

After obtaining the entire system model, the next objective is to add a random noise to the captured measurements. This is done using function "*randn*" in MATLAB®. Here, 10 percent noise has been added to the captured measurements. This is done so that simulation of actual nature of measurements from the real time data acquisition system can be carried out.

A sample of noise added to load angle δ of synchronous generator 2 has been shown:

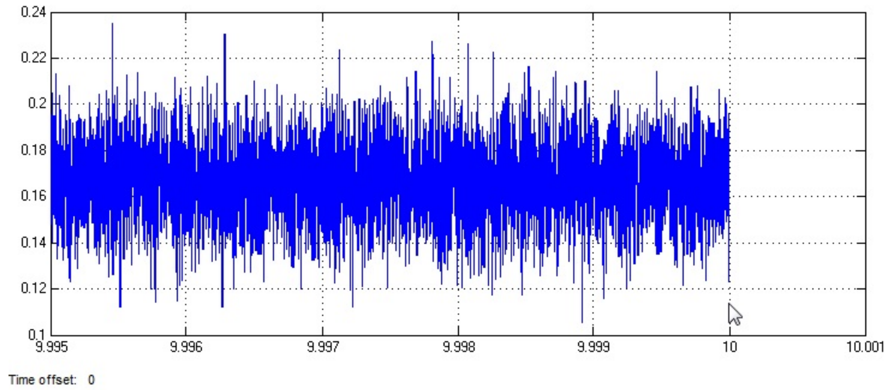

Figure 3.14: 10 percent noise added to load angle of synchronous generator 2

Likewise, noise has been added to other captured measurements as well.

3.4 EKF Implementation

After adding noise to parameters, the next objective is to eliminate this noise effect from the measured signal and estimate the main states of the system accurately. This estimation is carried out using EKF technique.

3.4.1 System Modeling for EKF Application to WSCC 3-Generator, 9-Bus System

Considering the following states:

1. Rotor Angle (δ)
2. Rotor Speed (ω)
3. Mechanical Power (P_m)
4. Inertia Constant (H)
5. Damping Factor (D)
6. Transient Reactance (X_d')

Here, the voltage magnitude and the voltage phase angle are considered as measurements.

EKF estimator is designed such that it is capable of estimating these states accurately along with eliminating the effect of noise from the measurement signal. As EKF gives information regarding the next step estimation based on the information of the previous step state estimate, the system can be modelled as follows:

$$\delta_{k+1} = \delta_k + (\omega_k - \omega_0)\Delta t + w_1 \tag{3.17}$$

$$\omega_{k+1} = \omega_k + \frac{\omega_0}{2H_k}(P_{m,k} - P_{e,k})\Delta t + D_k(\omega_k - \omega_0)\Delta t + w_2 \tag{3.18}$$

$$P_{m,k+1} = P_{m,k} + w_3 \tag{3.19}$$

$$H_{k+1} = H_k + w_4 \tag{3.20}$$

$$D_{k+1} = D_k + w_5 \tag{3.21}$$

$$X'_{d,k+1} = X'_{d,k} + w_6 \tag{3.22}$$

where w_i represents the noise, ω_0 is the nominal frequency and Δt is the time step. Thus, using the equations 3.17, 3.18, 3.19, 3.20, 3.21 and 3.22, the Jacobian Process Matrix is given by:

$$A = \begin{bmatrix} 1 & \Delta t & 0 & 0 & 0 & 0 \\ 0 & 1 - \frac{D\omega_0\Delta t}{2H} & \frac{\omega_0\Delta t}{2H} & A_{24} & A_{25} & 0 \\ 0 & 0 & 1 & 0 & 0 & 0 \\ 0 & 0 & 0 & 1 & 0 & 0 \\ 0 & 0 & 0 & 0 & 1 & 0 \\ 0 & 0 & 0 & 0 & 0 & 1 \end{bmatrix} \tag{3.23}$$

where

$$A_{24} = [\frac{P_m - P_e - D(\omega - \omega_0)}{2H^2}]\omega_0\Delta t \tag{3.24}$$

$$A_{25} = [\frac{-(\omega - \omega_0)}{2H}]\omega_0\Delta t \tag{3.25}$$

where ω = rotor speed in rad/sec, $\omega_1 = 30$, $\omega_2 = 60$, $\omega_3 = 60$.

$\omega_0 = 377$ rad/sec for 60 hz frequency.

$\frac{D_1\omega_0}{2H_1} = 0.1$, $\frac{D_2\omega_0}{2H_2} = 0.2$, $\frac{D_3\omega_0}{2H_3} = 0.3$

Now for machine 1, 2 and 3, the system parameters which define its dynamics can be calculated using the below equations. The data for these calculations have been obtained from simulation and are presented in the below table:

Table 3.7: Data Required For Calculation

Parameter	Machine 1	Machine 2	Machine 3
P_G	0.716	1.63	0.85
Q_G	0.27	0.067	-0.109
V	1.04	1.025	1.025
X_q	0.0969	0.8645	1.2578
$X_q^{'}$	0.0969	0.1969	0.25

Rest of the data required are provided in table 3.4. So substituting the above data in the following equations:

Step 1:

$$I_G \exp^{j\gamma} = \frac{P_G - Q_G}{\bar{V}^*} \tag{3.26}$$

Step 2:

$$\delta = Angle\ \ of((Ve^{j\theta} + (R_s + jX_q)I_G e^{j\gamma})) \tag{3.27}$$

Step 3:

$$I_d + I_q = I_G e^{j\gamma} e^{-j(\delta - \pi/2)} \tag{3.28}$$

Step 4:

$$V_d + V_q = Ve^{j\theta} e^{-j(\delta - \pi/2)} \tag{3.29}$$

Step 5:

$$E_d^{'} = (X_q - X_q^{'})I_q \tag{3.30}$$

$$E_q^{'} = V_q + R_s I_q + X_d^{'})I_d \tag{3.31}$$

Step 6:

$$E_{fd} = E_q^{'}(X_d - X_d^{'})I_d \tag{3.32}$$

The mechanical input P_m is calculated as:

$$P_m = E_d^{'} I_d + E_q^{'} I_q + (X_q^{'} - X_d^{'}) I_d I_q \tag{3.33}$$

Finally, the result for P_m for three machines are obtained as: $P_{m1} = 0.716$ pu , $P_{m2} = 1.63$ pu and $P_{m3} = 0.85$ pu.

The input power (P_e) can be calculated as:

$$P_e = \frac{EV}{X} sin\delta \tag{3.34}$$

$P_{e1} = 7.507$p.u., $P_{e2} = 1.201$ p.u. and $P_{e3} = 0.79$ p.u.

Finally, substituting all the above results in equation 3.24, 3.25 and 3.23, the Jacobian Process Matrix for the three machines obtained are:

For Machine 1:

$$A_1 = \begin{bmatrix} 1 & \Delta t & 0 & 0 & 0 & 0 \\ 0 & 1 - 0.1\Delta t & 8\Delta t & -0.823\Delta t & 2776\Delta t & 0 \\ 0 & 0 & 1 & 0 & 0 & 0 \\ 0 & 0 & 0 & 1 & 0 & 0 \\ 0 & 0 & 0 & 0 & 1 & 0 \\ 0 & 0 & 0 & 0 & 0 & 1 \end{bmatrix} \tag{3.35}$$

For Machine 2:

$$A_2 = \begin{bmatrix} 1 & \Delta t & 0 & 0 & 0 & 0 \\ 0 & 1 - 0.2\Delta t & 29.5\Delta t & 11.88\Delta t & 9351.5\Delta t & 0 \\ 0 & 0 & 1 & 0 & 0 & 0 \\ 0 & 0 & 0 & 1 & 0 & 0 \\ 0 & 0 & 0 & 0 & 1 & 0 \\ 0 & 0 & 0 & 0 & 0 & 1 \end{bmatrix} \tag{3.36}$$

For Machine 3:

$$A_3 = \begin{bmatrix} 1 & \Delta t & 0 & 0 & 0 & 0 \\ 0 & 1-0.3\Delta t & 62.6\Delta t & 32.838\Delta t & 19844.2\Delta t & 0 \\ 0 & 0 & 1 & 0 & 0 & 0 \\ 0 & 0 & 0 & 1 & 0 & 0 \\ 0 & 0 & 0 & 0 & 1 & 0 \\ 0 & 0 & 0 & 0 & 0 & 1 \end{bmatrix} \tag{3.37}$$

Finally, the entire Jacobian Process Matrix for the system will be:

$$A = \begin{bmatrix} A_1 & 0 & 0 \\ 0 & A_2 & 0 \\ 0 & 0 & A_3 \end{bmatrix} \tag{3.38}$$

Now, the Measurement matrix which is also known as Measurement Jacobian is given by:

$$H = \begin{bmatrix} \frac{\partial V}{\partial \delta} & \frac{\partial V}{\partial \omega} & \frac{\partial V}{\partial P_m} & \frac{\partial V}{\partial H} & \frac{\partial V}{\partial D} & \frac{\partial V}{\partial X_d^{'}} \\ \frac{\partial \theta}{\partial \delta} & \frac{\partial \theta}{\partial \omega} & \frac{\partial \theta}{\partial P_m} & \frac{\partial \theta}{\partial H} & \frac{\partial \theta}{\partial D} & \frac{\partial \theta}{\partial X_d^{'}} \end{bmatrix} = \begin{bmatrix} 0 & 0 & 0 & 0 & 0 & \frac{\partial V}{\partial X_d^{'}} \\ 1 & 0 & 0 & 0 & 0 & \frac{\partial \theta}{\partial X_d^{'}} \end{bmatrix} \tag{3.39}$$

where

$$\frac{\partial V}{\partial X_d^{'}} = \frac{((-Q_e E^2 - 2X_d^{'} P_e^2)/\sqrt{f_1}) - 4Q_e}{\sqrt{f_2}} \tag{3.40}$$

$$\frac{\partial \theta}{\partial X_d^{'}} = \frac{2P_e f_2 - P_e X_d^{'}(((-4Q_e E^2 - 8X_d^{'} P_e^2)/\sqrt{f_1}) - 4Q_e)}{f_2\sqrt{E^2 f_2 - 4P_e^2 X_d^{'2}}} \tag{3.41}$$

and

$$f_1 = -4Q_e X_d^{'} E^2 + E^4 - 4P_e^2 X_d^{'} \tag{3.42}$$

$$f_2 = 2\sqrt{f_1} + 2E^2 - 4Q_e X_d^{'} \tag{3.43}$$

3.5 Summary

The various results obtained by simulating the WSCC model has been presented in this chapter. The comparison between the actual and the simulated data has been carried out which gives an exact scenario of the errors occurred during simulation. Also, it includes the state space model for the system with and without renewable energy source integrated and its analysis. Also, system modeling for EKF has been implemented to the conventional WSCC 3-generator 9-bus system. The complete system has been modeled and can be effectively used to estimate dynamic states on availability of system integration test results.

Chapter 4

Conclusion And Future Scope

The thesis highlights the issue that present state estimation technique based on SCADA which is static in nature is not accurate and it causes a serious burden on the system operators to make decisions at a faster rate. After evaluating the literature available for state estimation, it can be definitely concluded that dynamic state estimation is superior to the static state estimation. Therefore, a major emphasis has been given to dynamic state estimation in this dissertation work.

In the following sections, some conclusion has been made from the obtained results and a scope for future work is provided which is not addressed in this dissertation work due to certain complexities.

4.1 Conclusion

For the understanding of dynamic state estimation and its techniques, the WSCC 3-generator 9-bus system has been used as the base model. The state space model of the system with and without renewable energy has been obtained which gives an exact scenario of the dynamics of the system and its behaviour. The simulation performed on the system gives the measurements and to know the actual behaviour of the measurements available, some amount of random noise has been added to these measurements. The results obtained are not as desired as complete system modelling has not been taken into consideration but a near accurate results have been presented.

4.2 Future scope of work

The available literature does not indicate the dynamic state estimation of power system having large renewable penetration. An attempt has been made to model a system, however the efficacy of such model needs to be evaluated.

References

[1] Amit Jain and Shivkumar N.R., *"Power System Tracking And Dynamic State Estimation"*,IEEE 2009.

[2] Amit Jain and Shivkumar N.R., *"Phasor Measurements In Dynamic State Estimation Of Power Systems"*, Report No: IIIT/TR/2009/44, Centre for Power Systems International Institute Of Information Technology Hyderabad - 500 032, India, March 2009

[3] Jun Zhu and Ali Abur, *"Bad Data Identification When Using Phasor Measurements"*, IEEE.

[4] Benjamin Genet and Jean-Claude Maun, *"Voltage-Stability Monitoring Using Wide-Area Measurement Systems"*, Paper ID- 392, IEEE.

[5] A.K. Sinha and J.K. Mondal, *"Dynamic State Estimator Using ANN Based Bus Load Prediction"*, IEEE Transactions On Power System, Vol. 14, No. 4, November 1999.

[6] Huang, Yih-Fang, Stefan Werner, Jing Huang, Neelabh Kashyap, and Vijay Gupta. *"State Estimation in Electric Power Grids: Meeting New Challenges Presented by the Requirements of the Future Grid"*, IEEE Signal Processing Magazine, 2012.

[7] Zhenyu Huang, Kevin Schneider and Jarck Nieplocha,*"Feasibility Studies Of applying Kalman Filter Techniques to Power System Dynamic State Estimation"*, The 8th International Power Engineering Conference, IPEC 2007.

[8] *"A Guidebook for Minigrids"*-SERC LBNL March 2013(1).pdf

[9] P.M. Anderson and A.A. Fouad, *"Power System Control And Stability"*, Iowa State University Press, Ames, IA ,1977 .

[10] P. Sauer and M.A. Pai, *"Power System Dynamics And Stability"*, Prentice Hall Inc.,1998.

[11] Milano Federico, Documentation for PSAT, version 2.1.6, 2011.

[12] Slobodan Pajic *"Power System State Estimation and Contingency Optimal Power Flow-A Numerically Robust Implementation"* www.wpi.edu/Pubs/ETD/Available/Phddissertation.pdf.

[13] *"State Estimation in Electric Power Grids"* ee.nd.edu/faculty/vgupta/research/publications/hwhkg12.pdf.

[14] Salvador Alepuz, Member IEEE, Sergio Busquets-Monge, Student Member, IEEE, *"Interfacing Renewable Energy Sources to the Utility Grid Using a Three-Level Inverter"*, IEEE 2009.